

Stable Isotope-Labeled RNA Phosphoramidites to Facilitate Dynamics by NMR

Christoph H. Wunderlich^{*,1}, Michael A. Juen^{*,1}, Regan M. LeBlanc^{†,1}, Andrew P. Longhini^{†,1}, T. Kwaku Dayie^{†,1,2}, Christoph Kreutz^{*,1,2}

^{*}Institute of Organic Chemistry and Center for Biomolecular Sciences Innsbruck, University of Innsbruck, Innsbruck, Austria

[†]Department of Chemistry and Biochemistry, Center for Biomolecular Structure and Organization, University of Maryland, College Park, Maryland, USA

¹*Disclosures:* CH Wunderlich none, MA Juen none, C Kreutz, none; RM LeBlanc none, AP Longhini none, TK Dayie, none.

²Corresponding authors: e-mail address: dayie@umd.edu; christoph.kreutz@uibk.ac.at

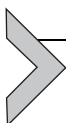
Contents

1. Theory	462
2. Equipment	463
3. Materials	464
3.1 Solutions and Buffers	466
4. Protocol	467
4.1 Duration	467
4.2 Preparation	467
4.3 Caution	467
5. Step 1: Synthesis of 6- ¹³ C-Uridine TOM Phosphoramidite	468
5.1 Overview	468
5.2 Duration	468
6. Step 2: Synthesis of 6- ¹³ C-Cytidine TOM Phosphoramidite	473
6.1 Overview	473
6.2 Duration	473
7. Step 3: Chemical RNA Synthesis	477
7.1 Overview	477
7.2 Duration	479
8. Step 4: Applications	484
8.1 Overview	484
8.2 Segmental Stable Isotope Labeling Using Chemically Synthesized RNAs	484
8.3 ¹³ C CPMG RD NMR Spectroscopy	485
8.4 ¹³ C ZZ Exchange NMR Spectroscopy	487
8.5 Chemical Exchange Saturation Transfer	488

9. Conclusions	490
Acknowledgments	491
References	492

Abstract

Given that Ribonucleic acids (RNAs) are a central hub of various cellular processes, methods to synthesize these RNAs for biophysical studies are much needed. Here, we showcase the applicability of 6-¹³C-pyrimidine phosphoramidites to introduce isolated ¹³C-¹H spin pairs into RNAs up to 40 nucleotides long. The method allows the incorporation of 6-¹³C-uridine and -cytidine residues at any desired position within a target RNA. By site-specific positioning of the ¹³C-label using RNA solid phase synthesis, these stable isotope-labeling patterns are especially well suited to resolve resonance assignment ambiguities. Of even greater importance, the labeling pattern affords accurate quantification of important functional transitions of biologically relevant RNAs (e.g., riboswitch aptamer domains, viral RNAs, or ribozymes) in the μ s- to ms time regime and beyond without complications of one bond carbon scalar couplings. We outline the chemical synthesis of the 6-¹³C-pyrimidine building blocks and their use in RNA solid phase synthesis and demonstrate their utility in Carr Purcell Meiboom Gill relaxation dispersion, ZZ exchange, and chemical exchange saturation transfer NMR experiments.



1. THEORY

Ribonucleic acid (RNA) is well recognized as a central player in key biological processes such as signaling and gene regulation, catalysis, or viral infections (Blount & Breaker, 2006; Breaker, 2011; Coppins, Hall, & Groisman, 2007; Haller, Souliere, & Micura, 2011; Reining et al., 2013; Serganov & Nudler, 2013). NMR spectroscopy has made significant contributions in revealing molecular details underlying these processes (Al-Hashimi, 2007; Al-Hashimi & Walter, 2008; Campbell, Bouchard, Desjardins, & Legault, 2006; Dayie, 2012; Fürtig, Buck, Richter, & Schwalbe, 2012; Hennig, Williamson, Brodsky, & Battiste, 2001; Johnson & Hoogstraten, 2008; Kloiber, Spitzer, Tollinger, Konrat, & Kreutz, 2011; Latham, Brown, McCallum, & Pardi, 2005; Mittermaier & Kay, 2009; Rinnenthal et al., 2011; Wenter, Reymond, Auweter, Allain, & Pitsch, 2006; Zhang, Sun, Watt, & Al-Hashimi, 2006). The first mandatory step to study both structure and dynamics of biomacromolecules is the introduction of a stable isotope-labeling pattern (Dayie, 2008; Hennig et al., 2001; Lu, Miyazaki, & Summers, 2010). Currently, enzymatic methods to introduce uniformly ¹³C- and/or ¹⁵N-labeled nucleotides into RNA and DNA are state-of-the-art (Hennig et al., 2001; Milligan, Groebe,

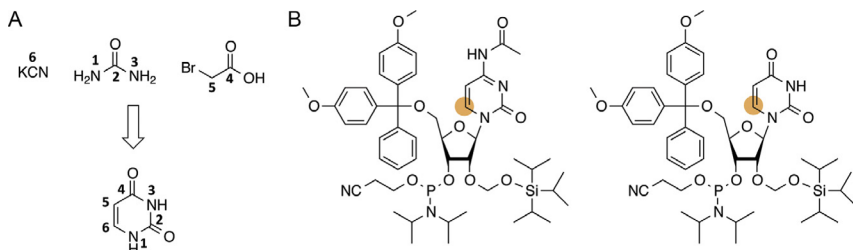


Figure 1 (A) All heteronuclei can be addressed for stable isotope labeling in uracil by choosing the appropriate precursor compounds. (B) 6-¹³C-cytidine (left) and -uridine (right) triisopropylsilyl-oxymethyl-protected RNA phosphoramidites. Orange (gray in the print version) circle: ¹³C.

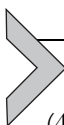
Witherell, & Uhlenbeck, 1987; Milligan & Uhlenbeck, 1989). Using these methods, nucleotide-specific-labeling patterns (i.e., only adenosines/uridines or guanosines/cytidines) can be applied in a straightforward manner by mixing labeled and unlabeled (deoxy-) ribonucleotide triphosphates (rNTPs) in polymerase-catalyzed reactions. However, the nature of the stable isotope-labeling pattern can limit the type of NMR experiments that can be run (Wunderlich et al., 2012). An isolated X-¹H (X = ¹³C or ¹⁵N) spin topology is particularly important for obtaining accurate parameters from the very powerful relaxation dispersion (RD) and chemical exchange saturation transfer (CEST) NMR experiments that address μs- to ms RNA dynamics. Our labeling strategy eliminates the deleterious strong homonuclear scalar coupling and therefore provides artifact-free dispersion profiles. Here, we outline a robust synthetic access to selectively labeled 6-¹³C-pyrimidine RNA phosphoramidites using any combination of the following: ¹⁵N1, ¹⁵N3, and ¹³C2 from ¹³C-¹⁵N-labeled urea; ¹³C4 and ¹³C5 from ¹³C-labeled bromoacetic acid; and ¹³C6 from K¹³CN (Fig. 1A and B).



2. EQUIPMENT

- 0.22-μm cellulose acetate filters
- 2-ml Eppendorf tubes
- 600/800 MHz NMR instrument equipped with ¹H/¹³C/³¹P probe with gradients
- Analytical Dionex DNAPac PA-100 column 4 × 250mm
- Balloons with a wall thickness of at least 0.3 mm
- Bent adapters with NS-stopcocks
- C18 SepPak cartridges (Waters)
- Dewar
- DNA/RNA synthesizer

Freezer at -20°C
Glass chromatography columns
High-pressure liquid chromatography system with a column oven
(e.g., Thermo Fisher Ultimate 3000)
High vacuum rotary vane pump
Magnetic stirrer with heating and an oil bath or heat block
Magnetic stirring bar
Medium pressure liquid chromatography system (e.g., ÄKTA start)
NMR tubes (5 or 3 mm) suitable for 600 and 800 MHz NMR
spectrometer
Parafilm
pH meter and electrode
Reflux condenser
Rotary evaporator with a diaphragm pump
Round-bottom flasks with volumes ranging from 25 to 1000 ml
Semipreparative Dionex DNAPac PA-100 column $9 \times 250\text{mm}$
Separatory funnel
Silica thin layer chromatography plates with fluorescence indicator
Suction filter
Syringes (1, 10, 20, and 50 ml volume)
UV/vis spectrophotometer
UV/vis cuvettes



3. MATERIALS

(4,4'-Dimethoxytriphenyl)methyl chloride (DMT-Cl)
[(Triisopropylsilyl)oxy]methyl chloride (TOM-Cl)
1-*O*-Acetyl-(2',3',5'-*O*-tribenzoyl)- β -D-ribofuranose (ATBR)
1,2-Dichloroethane
1*H*-benzylthiotetrazole
2-Cyanoethyl *N,N*-diisopropylchlorophosphoramidite
2,4,6-Triisopropylbenzenesulfonyl chloride (TPS-Cl)
28% Aqueous ammonia solution
4-(Dimethylamino)pyridine (DMAP)
Acetic acid
Acetic anhydride
Acetonitrile anhydrous
Acetonitrile DNA synthesis grade

Argon
Bis(trimethylsilyl)acetamide
CDCl₃
Celite
Citric acid
D₂O
Dibutyltin dichloride (or alternatively: di-*tert*-butyltin dichloride)
Dichloroacetic acid
Dimethylformamide anhydrous
Ethanol
Ethyl acetate
Hexanes (mixture of isomers)
Iodine
Methanol
Methylamine solution in ethanol (8 M)
Methylamine solution in water (30%)
Methylene chloride
Molecular sieve (4 Å)
N-methyl-2-pyrrolidone
N,N-diisopropylethylamine (DIPEA)
N,N-dimethylethylamine (DMEA)
Pyridine anhydrous
RNA support for solid phase synthesis (e.g., Custom primer support from GE healthcare)
Silica gel for column chromatography pore size 60 Å, ≥440 mesh particle size
Sodium acetate trihydrate
Sodium bicarbonate
Sodium perchlorate hydrate
Sodium sulfate anhydrous
Sym-collidine
Tetrabutylammonium fluoride trihydrate (TBAF)
Tetrahydrofuran (containing butylhydroxytoluene (BHT) as stabilizer)
Toluene
Triethylamine
Trimethylsilyl trifluoromethylsulfonate (TMSOTf)
Trizma base
Unlabeled [(triisopropylsilyl)oxy] methyl (TOM) protected RNA phosphoramidites (e.g., from ChemGenes)

Uracils (unlabeled and in various stable isotope-labeled forms by chemical synthesis)

Urea

3.1 Solutions and Buffers

Saturated sodium bicarbonate solution:

Add 200 g sodium bicarbonate to 1000 ml deionized water.

5% Citric acid

Dissolve 50 g citric acid in 1000 ml deionized water.

Cap A solution:

Dissolve 5 g DMAP in 50 ml acetonitrile.

Cap B solution:

Mix 25 ml acetonitrile with 10 ml acetic anhydride and 15 ml *sym*-collidine.

Oxidation solution:

Dissolve 250 mg iodine in 25 ml tetrahydrofuran. Then add 10 ml pyridine and 5 ml deionized water.

Detritylation solution:

Mix 10 ml dichloroacetic acid with 240 ml 1,2-dichloroethane.

100 mM sodium acetate solution:

Dissolve 13.6 g sodium acetate trihydrate in 1000 ml HPLC grade water.

Dionex column buffer A:

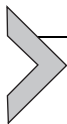
Component	Final concentration	Stock	Amount
Tris-HCl buffer, pH 8.0	25 mM	250 mM	100 ml
urea	6 M	-	360 g

Add water to 1-l. filter through 0.22- μ m hydrophilic membrane.

Dionex column buffer B:

Component	Final concentration	Stock	Amount
Tris-HCl buffer, pH 8.0	25 mM	250 mM	100 ml
urea	6 M	-	360 g
Sodium perchlorate hydrate	500 mM	-	70.2 g

Add water to 1-l filter through 0.22- μ m hydrophilic membrane.



4. PROTOCOL

4.1 Duration

Preparation	1–3 weeks
Step 1	5–7 days
Step 2	5–7 days
Step 3	5–7 days
Step 4	3 days

4.2 Preparation

Uracils with various stable isotope-labeling patterns are accessible via chemical synthesis as reported earlier (Alvarado, Longhini, et al., 2014). Starting from potassium cyanide and 2-bromoacetic acid, the cyano acetylurea precursor is obtained. In the final step, uracil is formed under reductive reaction conditions using palladium on barium sulfate under a hydrogen atmosphere. Prepare this key intermediate using the previously reported methods to proceed directly with step 1 (Fig. 2).

Purchase the unlabeled TOM protected RNA and DNA phosphoramidites along with the synthesis reagents (e.g., water free (<5 ppm) acetonitrile, 1*H*-benzylthiotetrazole (BTT) from a commercial supplier (e.g., ChemGenes, Glen Research). It is advisable to carry out test oligonucleotide syntheses to optimize the coupling, oxidation, and capping steps. For that purpose, DNA oligonucleotide synthesis should be used before switching to the more expensive RNA phosphoramidite chemistry for fine-tuning.

4.3 Caution

Please check the safety data sheets of the synthesis reagents before starting. Some of these reagents are very hazardous and should be handled by experienced chemists with extreme care in a well-vented fume hood. Phosphoramidites are rather sensitive chemical compounds and are degraded in the presence of acids and water or elevated temperatures. Phosphoramidite solutions (prepared using water-free acetonitrile) should be stored over freshly activated molecular sieve and are stable for several weeks at -20°C .

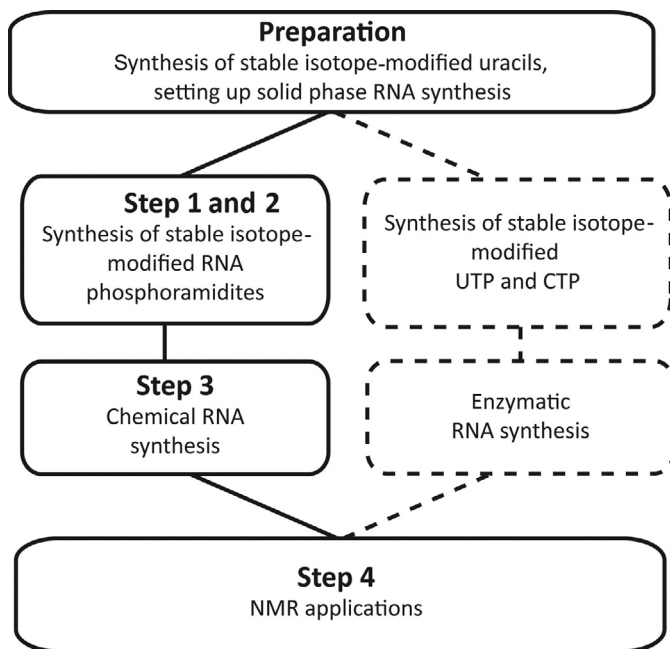


Figure 2 Workflow of the protocol. The part shown in dotted outline is an alternate extension to chemoenzymatic labeling using the selectively stable isotope-modified uracils (Alvarado, LeBlanc, et al., 2014; Alvarado, Longhini, et al., 2014).



5. STEP 1: SYNTHESIS OF 6-¹³C-URIDINE TOM PHOSPHoramidite

5.1 Overview

Transformations a, b, and c (Fig. 3) were reported earlier (Alvarado, Longhini, et al., 2014). Using the appropriate precursor composition, any heteronucleus of the uracil can be specifically enriched. The stable isotope-modified uracil key intermediate is coupled to a ribose building block under *Vorbrüggen* nucleosidation conditions (d) (Fig. 3). Subsequent removal of the benzoyl protecting groups (e) followed by tritylation (f) gives the precursor for the protection of the 2'-hydroxyl group using the TOM group (g) (Fig. 3). In the last step, the phosphoramidite is obtained (h) (Fig. 3).

5.2 Duration

5–7 days

- 1.1. Synthesis of 6-¹³C-2',3',5'-O-tribenzoyluridine: In a 100 ml round-bottom flask, suspend 6-¹³C-uracil (560 mg, 5 mmol) together with

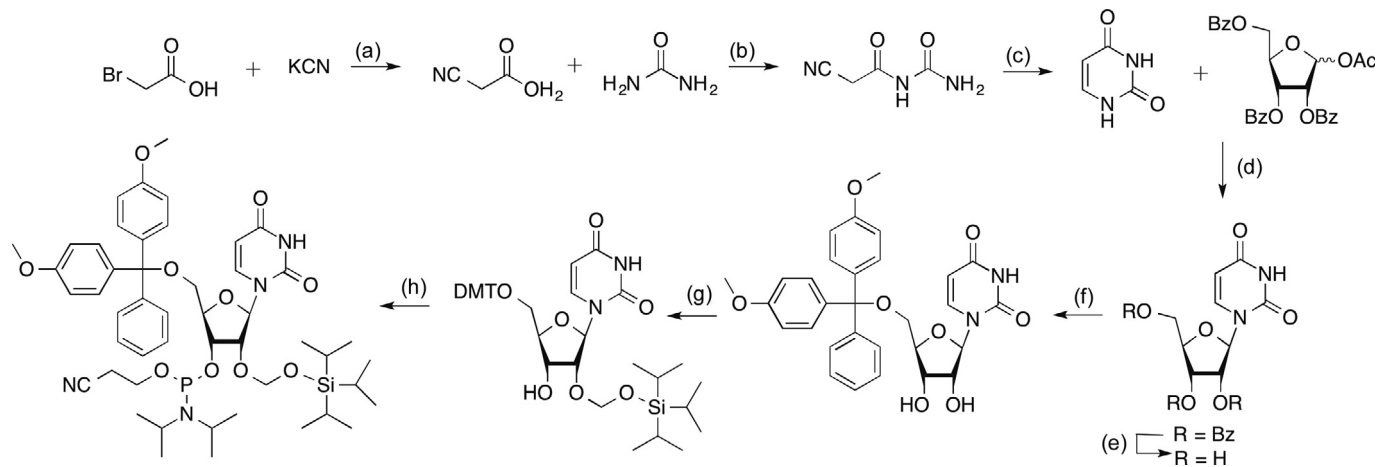


Figure 3 Synthetic access to 6-¹³C-uridine labeled fully protected RNA phosphoramidite.

- ATBR (2.5 g, 5 mmol) in 20 ml dry acetonitrile and evaporated to dryness. Repeat this procedure two times.
- 1.2. Add 20 ml dry acetonitrile and heat the suspension to 60 °C using a reflux condenser and an oil bath or a heat block.
 - 1.3. Then add bis(trimethylsilyl)acetamide (3.7 ml, 15 mmol) and stir the reaction mixture for 30 min at 60 °C. The suspension should turn into a clear solution.
 - 1.4. Finally, add TMSOTf (3.2 ml, 17.5 mmol) and continue stirring for another 30 min at 60 °C.
 - 1.5. The reaction progress can be monitored using TLC (ethyl acetate/hexanes 1/1, R_f (product) = 0.8).
 - 1.6. After that the reaction mixture is evaporated to yield an orange brown oil which is dissolved in methylene chloride and subsequently washed with saturated sodium bicarbonate solution. The organic phase is dried over sodium sulfate, filtered, and evaporated to dryness to give a yellow solid. The compound can be directly used in the next step.
 - 1.7. Synthesis of 6-¹³C-uridine: In a 100-ml round-bottom flask crude 6-¹³C-2',3',5'-O-tribenzoyluridine (2.5 g, 4.5 mmol) is dissolved in an ethanolic solution of methylamine (15 ml, 8 M) and an argon atmosphere and stirred at room temperature for 16 h.
 - 1.8. The reaction progress can be monitored using TLC (CH₂Cl₂/methanol 9/1, R_f (product) = 0.1).
 - 1.9. Then, the solution is evaporated to yield a yellow oil, which is dissolved in water and repeatedly extracted with methylene chloride to remove the *N*-methylbenzamide from the aqueous phase.
 - 1.10. The aqueous phase containing only 6-¹³C-uridine is then evaporated to dryness resulting in a yellow foam.
 - 1.11. To remove traces of impurities, recrystallization from ethanol is advisable.
 - 1.12. Synthesis of 5'-O-(4,4'-dimethoxytrityl)-6-¹³C-uridine: The product from the previous step (1.0 g, 4.1 mmol) is coevaporated three times with anhydrous pyridine in a 100-ml round-bottom flask.
 - 1.13. The residual oil is dissolved in 10 ml anhydrous pyridine. The reaction is carried out under an argon atmosphere. Add DMT (1.7 g, 5.0 mmol) in three portions within an hour.
 - 1.14. After 4 h at room temperature, the solvent is evaporated and coevaporated three times with toluene.

- 1.15. The orange foam is dried in high vacuum for 30 min and then dissolved in methylene chloride and washed with 5% citric acid, water, and saturated sodium bicarbonate solution.
- 1.16. The organic phase is dried over sodium sulfate, filtered, and evaporated to give the crude product.
- 1.17. The crude product is further purified by silica column chromatography using a gradient of methylene chloride and methanol (99/1 CH₂Cl₂/methanol to 95/5).
- 1.18. Synthesis of 5'-O-(4,4'-dimethoxytrityl)-2'-O-[[triisopropylsilyl]oxy]methyl]-6-¹³C-uridine: The tritylated uridine (616 mg, 1.13 mmol) is dissolved a mixture of DIPEA (765 μl, 4.5 mmol) and 1,2-dichloroethane (10 ml).
- 1.19. To the clear solution, dibutyltin dichloride (Bu₂SnCl₂; 616 mg, 2.02 mmol) is added, and the mixture is stirred for 1 h at room temperature.
- 1.20. Then, the solution is heated to 80 °C using a reflux condenser, and an oil bath or a heat block and TOM-Cl; 276 mg, 1.24 mmol) is added.
- 1.21. The reaction progress can be monitored using TLC (ethyl acetate/hexanes 1/1, R_f (product) = 0.6).
- 1.22. After 30 min, the reaction mixture is diluted with methylene chloride and the organic phase is washed with saturated sodium bicarbonate solution.
- 1.23. The organic phase is dried over sodium sulfate, filtered over Celite, and then evaporated to dryness.
- 1.24. The crude product is further purified by silica column chromatography using a gradient of hexanes and ethyl acetate (80/20 hexanes/ethyl acetate to 40/60).
- 1.25. Synthesis of 5'-O-(4,4'-dimethoxytrityl)-2'-O-[[triisopropylsilyl]oxy]methyl]-6-¹³C-uridine 3'-O-(2'-cyanoethyl N,N-diisopropylphosphoramidite): Anhydrous methylene chloride (5 ml) and DMEA (540 μl, 5.0 mmol) are mixed and then added to the product of the previous step (720 mg, 0.98 mmol).
- 1.26. The clear solution is stirred at room temperature for 15 min.
- 1.27. Add 2-cyanoethyl N,N-diisopropylchlorophosphoramidite (350 mg, 1.5 mmol) dropwise via a syringe and stir the reaction for 2 h.
- 1.28. The reaction progress can be monitored using TLC (ethyl acetate/hexanes 7/3 + 1% triethylamine, R_f (product) = 0.5).

- 1.29. The reaction mixture is then diluted with methylene chloride, and the organic phase is washed with half saturated sodium bicarbonate solution.
- 1.30. The organic phase is dried over sodium sulfate, filtered, and evaporated to dryness.
- 1.31. The crude product is further purified by silica column chromatography using a gradient of hexanes and ethyl acetate (50/50 hexanes/ethyl acetate to 40/60 + 1% triethylamine).
- 1.32. The quality of the final product should be checked by NMR spectroscopy (^1H , ^{13}C , and ^{31}P NMR in CDCl_3). The ^{31}P NMR spectrum consists of two peaks at 150.5 and 150.1 ppm (referenced to external 85% H_3PO_4). A ^{31}P peak at approximately 15 ppm indicates a phosphonate impurity, which needs to be removed by silica column chromatography to guarantee high coupling yields in the RNA solid phase synthesis.

5.2.1 Tip

The products of the respective steps should be characterized using NMR spectroscopy ($1\text{D-}^1\text{H}$ and ^{13}C spectra) and mass spectrometry and compared to data from literature before proceeding with the next step.

5.2.2 Tip

In the nucleosidation reaction (step 1.1), the temperature (60 °C) should be checked several times. Overheating will result in the formation of the undesired α -substituted uridine nucleoside.

5.2.3 Tip

In the nucleosidation reaction (step 1.3), let the solution cool to room temperature before adding TMSOTf to avoid a too vigorous reaction.

5.2.4 Tip

The extraction of *N*-methylbenzamide should be checked using silica TLC ($\text{CH}_2\text{Cl}_2/\text{MeOH}$ 9/1). After each extraction step, spot the aqueous phase and the organic phase on a silica TLC plate to check the composition of the phases. Normally, after three extraction steps no *N*-methylbenzamide is found in the aqueous phase.

5.2.5 Tip

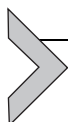
In the tomylation reaction (step 1.19), separation of organic and aqueous phase can be retarded especially when carrying out the reaction on a larger scale. In that case, the use of the bis-(*tert*-butyl)tin dichloride is recommended.

5.2.6 Tip

The tomylation reaction gives a distribution of desired 2'-*O*-regioisomer/undesired 3'-*O*-regioisomer/starting material of 1/1/1. To improve the yield, collect the 3'-*O*-regioisomer and remove the TOM protecting group using 1 *M* tetrabutylammonium fluoride in acetonitrile (1 ml/250 mg) and combine it with the starting material. This recovered material can then be reused in the tomylation reaction.

5.2.7 Tip

When carrying out the silica column chromatography of phosphoramidites, it is absolutely necessary to add 1% triethylamine to the eluents to avoid degradation of the amidites on the column. Triethylamine should also be added to the TLC solvent.



6. STEP 2: SYNTHESIS OF 6-¹³C-CYTIDINE TOM PHOSPHORAMIDITE

6.1 Overview

Starting from 5'-*O*-(4,4'-dimethoxytrityl)-2'-*O*-[[triisopropylsilyl]oxy]methyl]-6-¹³C-uridine, the 3'-hydroxyl group is protected using acetic anhydride (a) (Fig. 4). Using TPS-Cl, the O⁴ of uridine is activated as a leaving group and can be replaced with an amino group using an ammonium hydroxide solution (b) (Fig. 4). If desired, ¹⁵N-labeled ammonium chloride in combination with a base (e.g., K₂CO₃) can be used to introduce a ¹⁵N label at the exocyclic amino group at this stage. N-selective acetylation (c) and finally phosphitylation (d) yield the desired 6-¹³C-cytidine phosphoramidite (Fig. 4).

6.2 Duration

5–7 days

- 2.1. Synthesis of 3'-*O*-acetyl-5'-*O*-(4,4'-dimethoxytrityl)-2'-*O*-[[triisopropylsilyl]oxy]-methyl]-6-¹³C-uridine: In a 50-ml round-

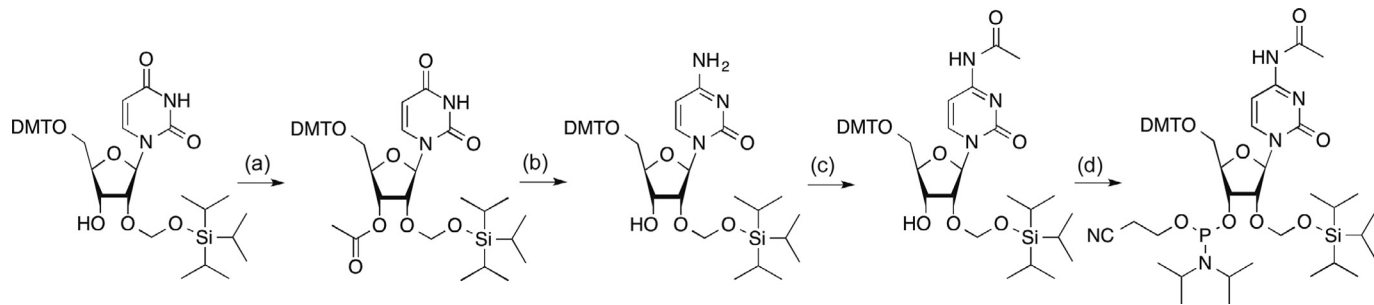


Figure 4 Synthetic access to 6-¹³C-cytidine labeled fully protected RNA phosphoramidite.

- bottom flask, 5'-O-(4,4'-dimethoxytrityl)-2'-O-[[triisopropylsilyl oxy]methyl]-6-¹³C-uridine (350 mg, 0.47 mmol) is dissolved in 1 ml anhydrous pyridine and is stirred at room temperature.
- 2.2. Add a catalytic amount of DMAP (5 mg, 0.05 mmol).
 - 2.3. Cool the reaction mixture to 0 °C and add acetic anhydride (48 µl, 0.51 mmol) dropwise.
 - 2.4. Remove the ice bath and continue stirring for 2 h.
 - 2.5. The reaction progress can be monitored using TLC (ethyl acetate/hexanes 1/1, R_f (product)=0.7).
 - 2.6. The solvent is evaporated, and the residue coevaporated twice with toluene.
 - 2.7. The residue is dissolved in methylene chloride, and the organic phase is washed with 5% citric acid, water, and saturated sodium bicarbonate solution.
 - 2.8. Dry the organic phase over sodium sulfate, filter, and evaporate to dryness.
 - 2.9. The crude product can directly be used in the next step.
 - 2.10. Synthesis of 5'-O-(4,4'-dimethoxytrityl)-2'-O-[[triisopropylsilyl oxy]-methyl]-6-¹³C-cytidine: Mix anhydrous methylene chloride (4 ml) and triethylamine (NEt₃, 528 µl, 3.8 mmol). To this mixture, add the crude product from the previous step (300 mg, 0.38 mmol) and DMAP (5 mg, 0.05 mmol).
 - 2.11. After 10 min, add TPS-Cl; (176 mg, 0.58 mmol) in small portions over a period of 1 h.
 - 2.12. Stir the reaction for another 4 h at room temperature.
 - 2.13. Dilute the reaction mixture with methylene chloride and wash the organic phase with half saturated sodium bicarbonate solution.
 - 2.14. Dry the organic phase over sodium sulfate, filter, and evaporate to dryness.
 - 2.15. Dry the resulting foam in high vacuum for 30 min.
 - 2.16. Dissolve the crude product from the previous step in 4 ml tetrahydrofuran and add 4 ml 28% aqueous ammonia solution. Continue stirring for 18 h at room temperature.
 - 2.17. After 18 h, evaporate the reaction mixture to yield an oily residue. Take up the residue in 4 ml ethanolic methylamine solution (8 M) and stir for 1 h.
 - 2.18. The reaction progress can be monitored using TLC (CH₂Cl₂/methanol 96/4, R_f (product)=0.45).

- 2.19. Evaporate the solvent and dry the residual oil in high vacuum.
- 2.20. Dissolve the oil in methylene chloride and wash the organic phase with saturated sodium bicarbonate solution.
- 2.21. Dry the organic phase over sodium sulfate, filter, and evaporate to dryness.
- 2.22. Purify the resulting foam from the previous step using silica column chromatography (CH₂Cl₂/methanol 99/1 to 95/5).
- 2.23. Synthesis of *N*⁴-acetyl-5'-*O*-(4,4'-dimethoxytrityl)-2'-*O*-[[[(triisopropylsilyl)-oxy]methyl]-6-¹³C-cytidine: Dissolve the product from the previous step (190 mg, 0.26 mmol) in 1 ml anhydrous dimethylformamide. Then add acetic anhydride (25 μl, 0.26 mmol) dropwise.
- 2.24. Stir the reaction for 22 h at room temperature.
- 2.25. The reaction progress can be monitored using TLC (ethyl acetate/hexanes 7/3, *R*_f (product) = 0.38).
- 2.26. Quench the reaction by the addition of a few drops of methanol.
- 2.27. Evaporate the solvent and dissolve the oily residue in methylene chloride.
- 2.28. Wash the organic phase with saturated sodium bicarbonate solution.
- 2.29. Dry the organic phase over sodium sulfate, filter, and evaporate to dryness.
- 2.30. Purify the crude product using silica column chromatography (CH₂Cl₂/methanol 99/1 to 98/2).
- 2.31. Synthesis of *N*⁴-acetyl-5'-*O*-(4,4'-dimethoxytrityl)-2'-*O*-[[[(triisopropylsilyl)-oxy]methyl]-6-¹³C-cytidine 3'-*O*-(2'-Ccyanoethyl *N,N*-diisopropylphosphoramidite): Anhydrous methylene chloride (5 ml) and DMEA (250 μl, 2.3 mmol) are mixed and then added to the product of the previous step (130 mg, 0.98 mmol).
- 2.32. The clear solution is stirred at room temperature for 15 min.
- 2.33. Add 2-cyanoethyl *N,N*-diisopropylchlorophosphoramidite (83 mg, 0.35 mmol) dropwise via a syringe and stir the reaction for 2 h.
- 2.34. The reaction progress can be monitored using TLC (ethyl acetate/hexanes 7/3 + 1% triethylamine, *R*_f (product) = 0.46).
- 2.35. The reaction mixture is then diluted with methylene chloride, and the organic phase is washed with half saturated sodium bicarbonate solution.
- 2.36. The organic phase is dried over sodium sulfate, filtered, and evaporated to dryness.

- 2.37.** The crude product is further purified by silica column chromatography using a gradient of hexanes and ethyl acetate (70/30 hexanes/ethyl acetate + 1% trimethylamine to 30/70 hexanes/ethyl acetate + 1% triethylamine).
- 2.38.** The quality of the final product should be checked by NMR spectroscopy (^1H , ^{13}C , and ^{31}P NMR in CDCl_3). The ^{31}P NMR spectrum should show two peaks at 150.8 and 150.6 ppm (referenced to external 85% H_3PO_4). A ^{31}P peak at approximately 15 ppm indicates a phosphonate impurity, which needs to be removed by silica column chromatography to guarantee high coupling yields in the RNA solid phase synthesis.

6.2.1 Tip

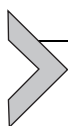
The products of the respective steps should be characterized using NMR spectroscopy (1D- ^1H and ^{13}C spectra) and mass spectrometry and compared to data from literature before proceeding with the next step.

6.2.2 Tip

The crude product from step 2.15 is not stable and should not be stored for a prolonged time at room temperature. It is best used directly after drying in high vacuum.

6.2.3 Tip

When carrying out the silica column chromatography of phosphoramidites, it is absolutely necessary to add 1% triethylamine to the eluents to avoid degradation of the amidites on the column. Triethylamine should also be added to the TLC solvent.



7. STEP 3: CHEMICAL RNA SYNTHESIS

7.1 Overview

Using an automated RNA/DNA synthesizer, the 6- ^{13}C -pyrimidine-modified TOM-protected RNA phosphoramidites can be introduced as site-specific stable isotope labels into a target RNA for NMR application. The phosphoramidite chemistry is well established and high-quality synthetic RNAs can be obtained (Fig. 5; Micura, 2002). The main advantage of the chemical oligonucleotide synthesis is that no sequence requirements,

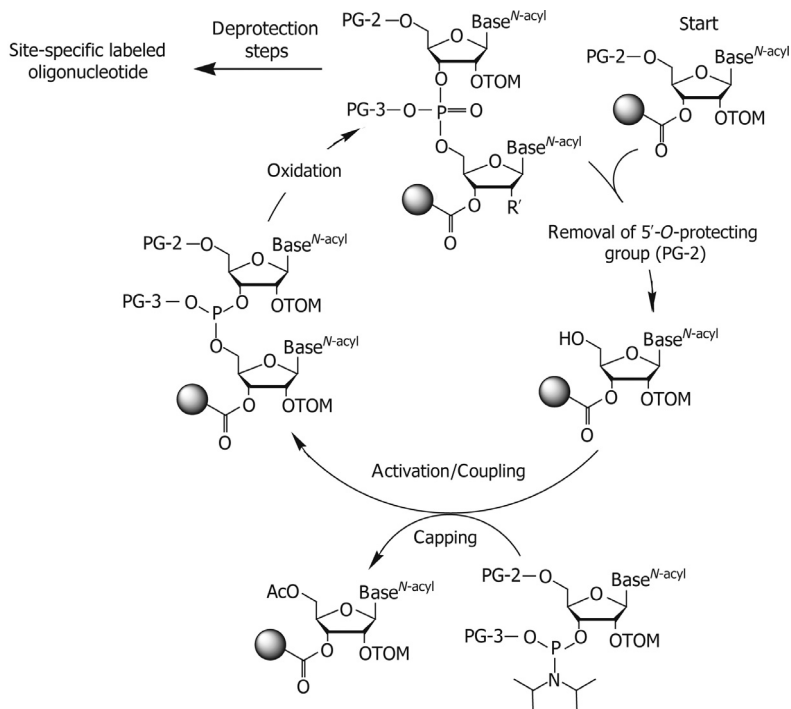


Figure 5 Oligonucleotide solid phase synthesis cycle: After removal of the trityl protecting group, the 5'-OH group is attached to the next building block in the activation/coupling step using a weak acid (e.g., 1*H*-benzylthiotetrazole) and the respective phosphoramidite. Unreacted 5'-hydroxyls are capped using acetic anhydride. In the final step, the P(III) species is oxidized to the more stable P(V) species before the next synthesis cycle is entered.

as e.g., in the case of T7 RNA polymerase assisted *in vitro* transcription, are encountered. Furthermore, the number and positioning of the stable modified phosphoramidites can be freely chosen. Several DNA/RNA synthesizers are commercially available (e.g., from Applied Biosystems, GE Healthcare, Bioautomation). As aforementioned in [Section 4.2](#), the synthesis cycle should be optimized before using stable isotope-modified RNA phosphoramidites.

Optimized synthesis cycles for an ABI 391 PCRmate are available on request from the authors. The assembled RNA sequence is then deprotected in a two-step procedure: (i) alkaline deprotection: releases the oligonucleotide from the solid support, removes the nucleobase protecting groups and the cyanoethyl groups; (ii) fluoride deprotection: using 1 *M*

tetrabutylammonium fluoride in tetrahydrofuran the TOM group is cleaved off. Finally, anion exchange chromatography is used to purify the stable isotope-modified RNA.

7.2 Duration

5–7 days

- 3.1. Freshly prepare phosphoramidite solutions: dissolve 1 g of each TOM protected phosphoramidite in 10 ml water-free acetonitrile (<5 ppm water) and add freshly activated molecular sieve.
- 3.2. Freshly prepare activator solution: dissolve 1*H*-benzylthiotetrazole (1.44 g) in 30 ml water-free acetonitrile and add freshly activated molecular sieve.
- 3.3. Fill a 1.3- μ mol synthesis column with the appropriate amount of solid support (e.g., 16 mg rA Custom Primer support, 80 μ mol g⁻¹, GE Healthcare).
- 3.4. Attach synthesis reagents (Cap A, Cap B, oxidation solution, detritylation solution, and water-free acetonitrile) to the appropriate ports on the RNA synthesizer. Attach phosphoramidite solutions (rA, rG, rC, U, and stable isotope-modified amidites to the additional ports X1, X2, etc.) to the appropriate ports on the RNA synthesizer.
- 3.5. Fill the reagent lines with the respective solution. Fill the phosphoramidite lines with a minimal volume of respective amidite solution to reduce loss (especially for the stable isotope-labeled phosphoramidites). Attach the synthesis column and wash the column with water-free acetonitrile to check for leaks.
- 3.6. Enter the target sequence and start the synthesis procedure.
- 3.7. Check the first detritylation step of the solid support. A deep red color should be observable.
- 3.8. Check the coupling of the first phosphoramidite by observing the detritylation step. Again a deep red color of the detritylation solution should be observed. Let the synthesis proceed until the sequence assembly is finished. If possible check the final detritylation step. A red color of the solution hints at a successful sequence synthesis.
- 3.9. Dry the solid support in high vacuum for 30 min. Transfer the solid support into a 1.5-ml Eppendorf® tube with a sealing.
- 3.10. Ethanolic methylamine/aqueous methylamine deprotection: Add 650 μ l aqueous methylamine solution (30%) and 650 μ l ethanolic methylamine solution (8 *M*) to the solid support and let stand for

- 6 h at room temperature. Vortex 1/h. Or alternatively: aqueous methylamine/aqueous ammonia (AMA) deprotection: Add 650 μ l aqueous methylamine solution (30%) and 650 μ l ammonium hydroxide solution (28%) and heat to 37 °C for 1.5 h.
- 3.11. Centrifuge to pellet the solid support on the bottom of the tube and transfer the supernatant to a 10-ml round-bottom flask. Wash the solid support three times with 1 ml tetrahydrofuran/water (1/1, v/v) and add the washings to the 10-ml round-bottom flask. Evaporate the solution in the flask to dryness and dry the residue in high vacuum for 30 min to remove the bases.
 - 3.12. Dissolve the residue in the 10-ml round-bottom flask in 1.6 ml 1 *M* tetrabutylammonium fluoride solution in tetrahydrofuran. If the residue does not readily dissolve, add 100 μ l *N*-methyl-2-pyrrolidone to obtain a clear solution. Stopper the 10-ml round-bottom flask tightly with the aid of Parafilm© and keep the deprotection solution at 33 °C for at least 14 h. Quench the 2'-*O*-deprotection reaction with 1.6 ml 1 *M* triethylammonium acetate solution. Evaporate the deprotection solution to an approximate volume of 1 ml.
 - 3.13. Load the crude RNA on a HiPrep desalting 26/10 column (GE Healthcare) using a MPLC system with UV and conductivity detection. Use HPLC grade water (18 *M* Ω cm) to elute the crude RNA. The RNA elutes first and can be identified by its high UV absorbance at 254 nm, whereas the later eluting salts lead to strong increase in conductivity. Collect the RNA in a 50-ml round-bottom flask. Evaporate the RNA containing fraction to dryness and redissolve the oligonucleotide in 1 ml HPLC grade water. The solution of the crude oligonucleotide product can be stored at -20 °C for several weeks without degradation (Fig. 6).
 - 3.14. To check the quality of the crude RNA, anion exchange chromatography using an analytical Dionex DNAPac PA-100 (4 \times 250 mm) column and buffer A and B on a HPLC system should be carried out. For RNAs comprising less than 20 nucleotides, a gradient from 0% to 40% B in A in 30 min is sufficient, and for larger RNAs, a gradient from 0% to 60% B in A in 45 min needs to be applied. The chromatographic analysis is carried out at 80 °C to fully denature the RNA (Fig. 7).
 - 3.15. To further purify the crude RNA semipreparative anion exchange chromatography on a Dionex DNAPac PA-100 (9 \times 250 mm) column using buffer A and B is carried out. The gradient needs to be

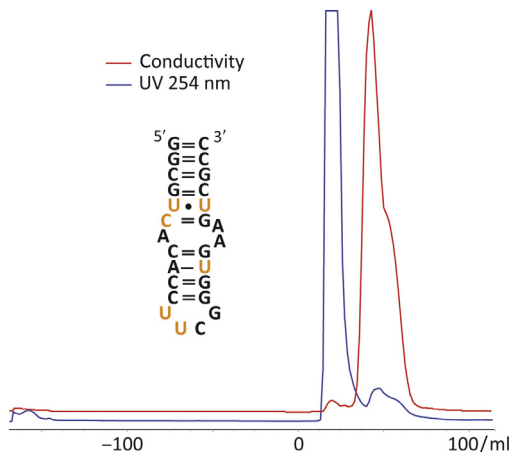


Figure 6 Desalting of crude RNA on a ÄKTA start system (GE Healthcare) using a HiPrep desalting column 26/10. $6\text{-}^{13}\text{C}$ -pyrimidine labels are highlighted in orange (gray in the print version).

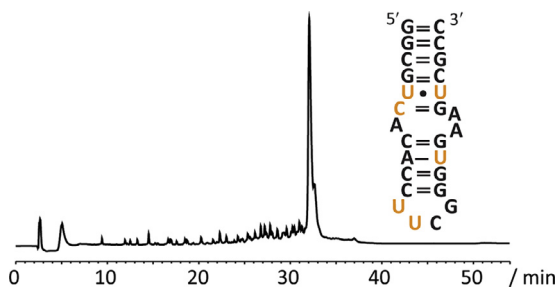


Figure 7 Anion exchange chromatographic analysis of a crude RNA comprising 27 nucleotides. The analysis was carried out on a Dionex DNAPac PA-100 column ($4 \times 250\text{mm}$) using a gradient of 0–60% buffer B in buffer A in 45 min at $80\text{ }^\circ\text{C}$. The UV absorbance trace at 260 nm is shown.

optimized for every target RNA and depends on its length and nucleotide composition. The chromatographic purification is carried out at $80\text{ }^\circ\text{C}$ to fully denature the RNA. Several runs (typically 5–6) loading approximately 30 nmol crude RNA per run are needed to purify the product of a RNA synthesis on a $1.3\text{ }\mu\text{mol}$ scale (Fig. 8).

- 3.16. Dilute the fractions containing desired RNA with an equal volume of 100 mM sodium acetate solution.

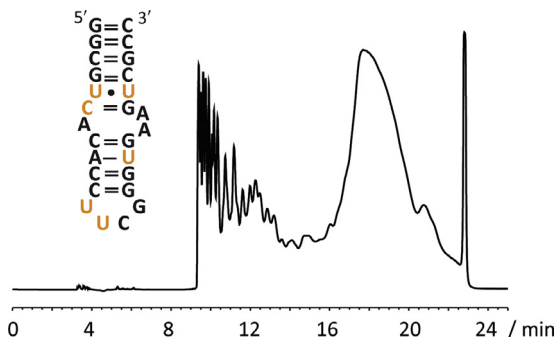


Figure 8 Anion exchange chromatographic purification of a crude RNA comprising 27 nucleotides. A gradient of 30–40% buffer B in buffer A in 15 min at 80 °C was used. The UV absorbance trace at 260 nm is shown.

- 3.17. Prepare a C18 SepPak cartridge (Waters): (i) 3 column volumes (CV) acetonitrile, (ii) 3 CV acetonitrile/water (1/1, v/v), (iii) 3 CV water, (iv) 3 CV 100 mM sodium acetate.
- 3.18. Then load the RNA containing fractions on the SepPak cartridge.
- 3.19. Elute the buffer salts by washing the RNA with 3 CV water.
- 3.20. Elute the RNA using 3 CV acetonitrile/water (1/1, v/v) into a 50-ml round-bottom flask.
- 3.21. Evaporate the solution containing the target RNA to dryness and redissolve the RNA in 1 ml HPLC grade water.
- 3.22. To check the quality of the purified RNA, anion exchange chromatography using an analytical Dionex DNAPac PA-100 (4 × 250 mm) column and buffer A and B on a HPLC system should be carried out. For RNAs comprising less than 20 nucleotides, a gradient from 0% to 40% B in A in 30 min should be used, for larger RNAs a gradient from 0% to 60% B in A needs to be applied. The chromatographic analysis is carried out at 80 °C to fully denature the RNA (Fig. 9).
- 3.23. The yield of purified target RNA can be calculated by applying the Beer–Lambert law:

$$c = A / (\epsilon^{260\text{nm}} l)$$

with c concentration in mol l^{-1} , A absorption at 260 nm, $\epsilon^{260\text{nm}}$ extinction coefficient at 260 nm in $\text{l mol}^{-1} \text{cm}^{-1}$ and l length of solution light passes in cm. The extinction coefficient $\epsilon^{260\text{nm}}$ of the RNA can be estimated by adding the $\epsilon^{260\text{nm}}$ values of the monomers.

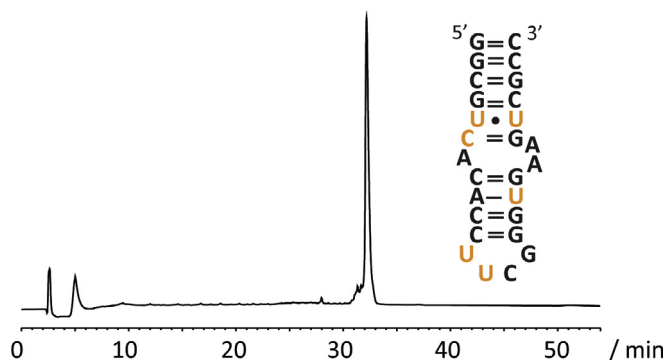


Figure 9 Anion exchange chromatographic analysis of a purified RNA comprising 27 nucleotides. The analysis was carried out on a Dionex DNAPac PA-100 column ($4 \times 250\text{mm}$) using a gradient of 0% to 60% buffer B in buffer A in 45 min at 80°C . The UV absorbance trace at 260 nm is shown. The purity is estimated by peak integration to be $>95\%$.

Nucleotide	$\epsilon^{260\text{nm}}$ [$\text{l mol}^{-1} \text{cm}^{-1}$]
rA	15,300
rC	7400
rG	11,700
U	9900

3.24. Lyophilize the desired amount of RNA for the NMR spectroscopic application.

7.2.1 Tip

Do not overfill the synthesis column with solid support as the growing RNA chain could clog the column.

7.2.2 Tip

If using the AMA procedure at elevated temperatures, allow cooling to room temperature before opening the tube to avoid spilling of the deprotection solution.

7.2.3 Tip

Use tetrahydrofuran containing the stabilizer BHT for the preparation of the TBAF solution. Stabilizer-free tetrahydrofuran can form radicals leading to irreproducible deprotection results.

7.2.4 Tip

The integrity and homogeneity of the purified RNA (from [step 3.21](#)) can further be checked using LC-ESI mass spectrometry and denaturing and native PAGE.



8. STEP 4: APPLICATIONS

8.1 Overview

Using these stable isotope-modified RNA phosphoramidites, an isolated ^1H - ^{13}C -spin pair is introduced which allows the application of Carr Purcell Meiboom Gill (CPMG) RD NMR experiments in a straightforward manner ([Wunderlich et al., 2012](#)). Additionally, a significant side benefit of this methodology is that the site selectively labeled nucleobase can be coupled enzymatically with ribose to make labeled rNTPs ([Alvarado, LeBlanc, et al., 2014](#); [Alvarado, Longhini, et al., 2014](#)). Importantly, this very powerful methodology can be exploited to detect and quantify important functional dynamics occurring on the μs - to ms time scale. Thus, structural transitions of RNA important for ligand binding or catalysis can be investigated readily. In this section, we discuss the potential of these chemically synthesized RNAs in a segmental isotope-labeling protocol to address functional dynamics in larger RNAs, as well as its incorporation using chemoenzymatic tricks.

We present ^{13}C CPMG RD data on a 27 nt RNA that mimics the bacterial 16S decoding site (A site), which is involved in discriminating cognate and near-cognate tRNAs ([Dethoff, Petzold, Chugh, Casiano-Negroni, & Al-Hashimi, 2012](#)). The labeling pattern is also well suited to study slower RNA secondary structure refolding kinetics occurring at exchange rates at 1 s^{-1} . We illustrate the applicability of the stable isotope-labeled RNAs in a ^{13}C ZZ exchange NMR experiment addressing the refolding kinetics between two hairpin folds, one representing the terminator and the other the antiterminator fold of the *Fsu* preQ₁ riboswitch system ([Rieder, Kreutz, & Micura, 2010](#)). Finally, we also showcase the usefulness to CEST experiments on a 48 nt RNA labeled with ^{13}C on the base chemically but coupled to the ribose enzymatically ([Alvarado, LeBlanc, et al., 2014](#); [Alvarado, Longhini, et al., 2014](#)).

8.2 Segmental Stable Isotope Labeling Using Chemically Synthesized RNAs

Segmental isotope labeling is the key methodology when studying high-molecular weight nucleic acid systems where spectral overlap dominates

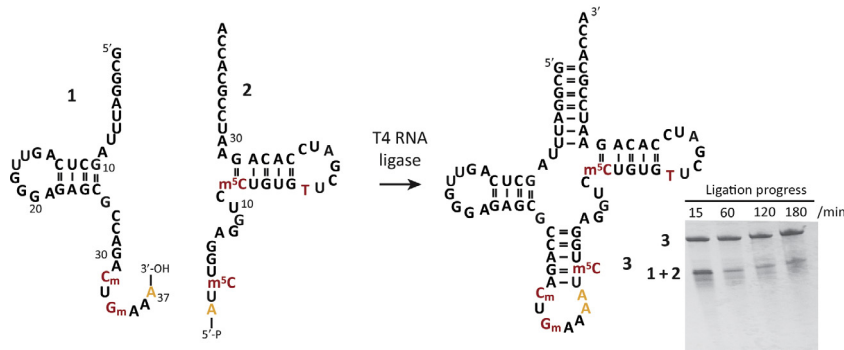
(Duss, Maris, von Schroetter, & Allain, 2010; Lebars et al., 2014; Lu, Miyazaki, & Summers, 2010; Nelissen et al., 2008; Tzakos, Easton, & Lukavsky, 2007). In short, a stable isotope-labeled RNA produced either by chemical or enzymatic methods is ligated to another (e.g., unlabeled) RNA giving access to larger constructs with a few NMR active residues to address structural and dynamic features. The procedure makes use of two enzymes, the T4 RNA ligase and T4 DNA ligase, but also deoxyribozymes were used to ligate two RNA strands (Dayie, 2008; Wawrzyniak-Turek & Höbartner, 2014). When using T4 RNA or DNA ligase a 5'-monophosphate is required on the donor strand and a 3'-hydroxyl group at the acceptor fragment. The T4 DNA ligase further needs a DNA splint as the enzyme catalyzes the joining of RNA to another RNA strand in a duplex molecule but will not join single-stranded nucleic acids. In contrast, T4 RNA ligase accepts single-stranded RNAs as substrates. Solid phase RNA synthesis is perfectly suited to craft oligonucleotides with the desired 5'-monophosphate (using a commercially available phosphorylation reagent) and 3'-OH, termini which are not directly accessible via *in vitro* transcription. For *in vitro* synthesis, a ribozyme sequence (e.g., hepatitis delta virus) must be appended at the 5'- and 3'-ends of the donor fragment RNA (Dayie, 2008; Kieft & Batey, 2004), and the 5'-diphosphate is cleaved enzymatically by RNA 5'-polyphosphatase to obtain the desired monophosphorylated group at the 5'-termini (Chen, Zuo, Wang, & Dayie 2012; Dayie, 2008).

We explored the applicability of chemically synthesized RNAs for segmental stable isotope labeling. Here, we showcase the tremendous potential of the approach by the ligation of two RNAs comprising ^{13}C -methyl modifications naturally occurring in transfer RNAs (Fig. 10). Ligation of a 39 nt acceptor and a 37 nt donor strand using T4 RNA ligase yielded a ^{13}C -methyl-modified phenylalanine tRNA. NMR studies on the dynamics of the ^{13}C -methyl-modified residues are currently carried out in our laboratories.

8.3 ^{13}C CPMG RD NMR Spectroscopy

The 27 nt A-site RNA was modified using 6- ^{13}C -uridine and 6- ^{13}C -cytidine phosphoramidites. The successful incorporation of the six stable isotope labels (five 6- ^{13}C -uridines and one 6- ^{13}C -cytidine) was confirmed by NMR spectroscopy. A standard heteronuclear single quantum correlation (HSQC) spectrum did show the expected six ^1H - ^{13}C -correlation peaks (Fig. 11A). We then addressed the previously reported conformational dynamics of this RNA using ^{13}C CPMG RD NMR spectroscopy

A



B

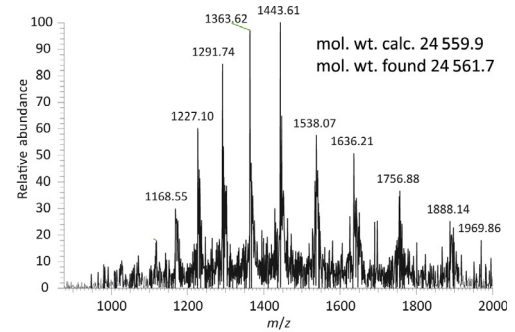


Figure 10 (A) One step T4 RNA ligase catalyzed joining of a 37 and 39 nt RNA comprising ¹³C-modified methyl residues (highlighted in red (darkgray in the print version), ligation site highlighted in orange (gray in the print version)) yielding a full length 76 nt tRNA^{Phe}. Ligation progress can be readily followed using denaturing polyacrylamide gel electrophoresis (see inset). (B) Electrospray Ionization mass spectrometric analysis of tRNA^{Phe} ligation product.

Table 1 Summary of Exchange Data Obtained from ^{13}C -CPMG RD Experiments of the A-Site RNA at 288 K

	$k_{\text{ex}}/\text{s}^{-1}$	$p_{\text{A}}/\%$ ^a	$p_{\text{B}}/\%$ ^a	$\Delta\delta(^{13}\text{C})/\text{ppm}$ ^b
Global parameters	1204 ± 256	98.1 ± 0.8	1.9 ± 0.8	
U6				2.42 ± 0.4
U95				0.87 ± 0.6

^a p_{A} refers to the ground state and p_{B} to the excited state population.

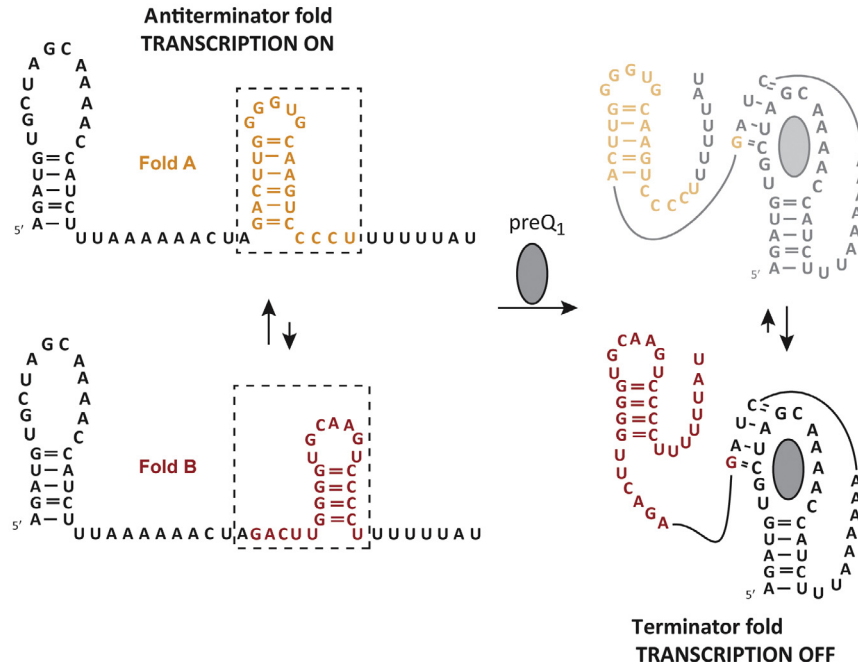
^b ^{13}C -chemical shift difference between ground state A and excited state B for the residues exhibiting nonflat dispersion profiles are given.

weight metabolites (Haller et al., 2011). We identified a bistable terminator antiterminator sequence partition (Fig. 12A, dashed box; Rieder et al., 2010). To address the equilibrium refolding kinetics of this naturally occurring bistable RNA element, a single 6- ^{13}C -cytidine substitution was introduced, and ^{13}C -longitudinal exchange NMR spectroscopy was applied. Integration of the ^1H - ^{13}C -correlation peaks in a standard HSQC spectrum yielded the equilibrium constant favoring fold B ($K_{\text{AB}}=3$). Subsequently, the forward and backward rates of the secondary structure equilibrium were determined at 33 °C using an approach introduced by analyzing longitudinal relaxation rates with and without exchange contribution (Fig. 12B). The forward rate constant k_{AB} amounts to $3.3 \pm 0.1 \text{ s}^{-1}$ and the rate k_{BA} for the folding process from state B to A to $1.4 \pm 0.3 \text{ s}^{-1}$.

8.5 Chemical Exchange Saturation Transfer

To characterize the nature of riboswitch RNA transitions on timescales slower than CPMG but faster than ZZ exchange, CEST experiments are carried out by varying the position of a very weak ^{13}C radiofrequency (rf) B_1 field and quantified indirectly using the intensities of the major state (NMR-visible) correlations (Bouvignies & Kay, 2012a,2012b; Fawzi, Ying, Ghirlando, Torchia, & Clore, 2011; Forsén & Hoffman, 1963; Longhini et al., 2015; Vallurupalli, Bouvignies, & Kay, 2012; Zhao, Hansen, & Zhang, 2014). As expected, when the B_1 field position coincides with or is close to the resonance frequency of the ^{13}C resonant peak in the ground state, the intensity of this ground state peak decreases because of rf saturation effect (Forsén & Hoffman, 1963). Significantly, when the weak B_1 field is applied close to the position of the corresponding peak from the excited (NMR-invisible) state, the

A



B

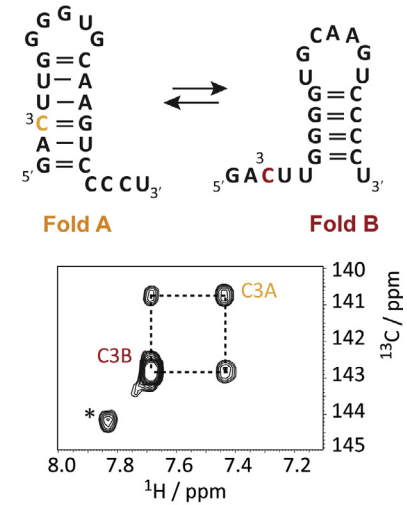


Figure 12 (A) Competing terminator antiterminator RNA folds and the influence of preQ₁ binding on the 2° structure equilibrium. (B) ¹³C longitudinal exchange spectrum at a mixing time of 200 ms and at 33 °C.

ground-state peak intensity also decreases due to the transfer of the rf perturbation from the excited state to the ground state by chemical exchange. A plot of the intensity of the ground-state (observed) peak as a function of the position of the B_1 field indicates a pair of dips, with the larger dip at the resonance frequency of the carbon in the ground state and the smaller dip at the frequency of the corresponding ^{13}C resonant peak in the excited state (Fig. 13). Thus, a visual inspection of the plotted data readily reveals that the NMR-invisible state is shifted into a carbon frequency region expected for residues in a Watson–Crick base-pair configuration (Fig. 13). Data were recorded at 16.4 T, and the CEST profiles were fitted using the Bloch–McConnell equations assuming a two-site exchange process (Longhini et al., 2015). Global fitting of CEST profile to a single two-state model resulted in $k_{\text{ex}} = 687 \pm 24 \text{ s}^{-1}$ and minor excited population $p_{\text{ES}} = 2.3 \pm 0.1\%$, and a ^{13}C -chemical shift difference between ground state and excited state of 3.3 ppm. With our selective labels, the large $^1J_{\text{C1}'\text{-C2}'}$ ($\sim 45 \text{ Hz}$) couplings do not complicate the measurements and need not be taken explicitly into account in the data analysis of sugar (C1') CEST profiles as required in previous studies using uniformly labeled RNA (Zhao et al., 2014).



9. CONCLUSIONS

Here, we presented a broad and versatile ^{13}C -labeling approach for RNA using 6- ^{13}C -pyrimidine phosphoramidite building blocks or chemoenzymatic coupling approach, which can be introduced into RNA by oligonucleotide solid phase or enzymatic synthesis. The 6- ^{13}C -pyrimidine labels are generally applicable to study conformational dynamics and the refolding kinetics in RNAs comprising up to 30–40 nucleotides using standard NMR techniques. For larger RNAs, the labeling protocol can be used in combination with enzymatic ligation strategies or chemoenzymatic approaches as outlined. In that case, pulse sequences comprising a TROSY element are particularly useful. The building blocks are currently used to site-specifically modify functional nucleic acids, such as riboswitch aptamer domains or ribozymes, to give fundamental insights into the functional dynamics of these RNAs. We anticipate that this methodology of incorporating modified or labeled nucleotides into specifically designated positions or regions of RNA is very general and will open up new avenues for not only studying the structure and dynamics of large RNAs but will also be useful in biotechnological applications such as RNA biosensors.

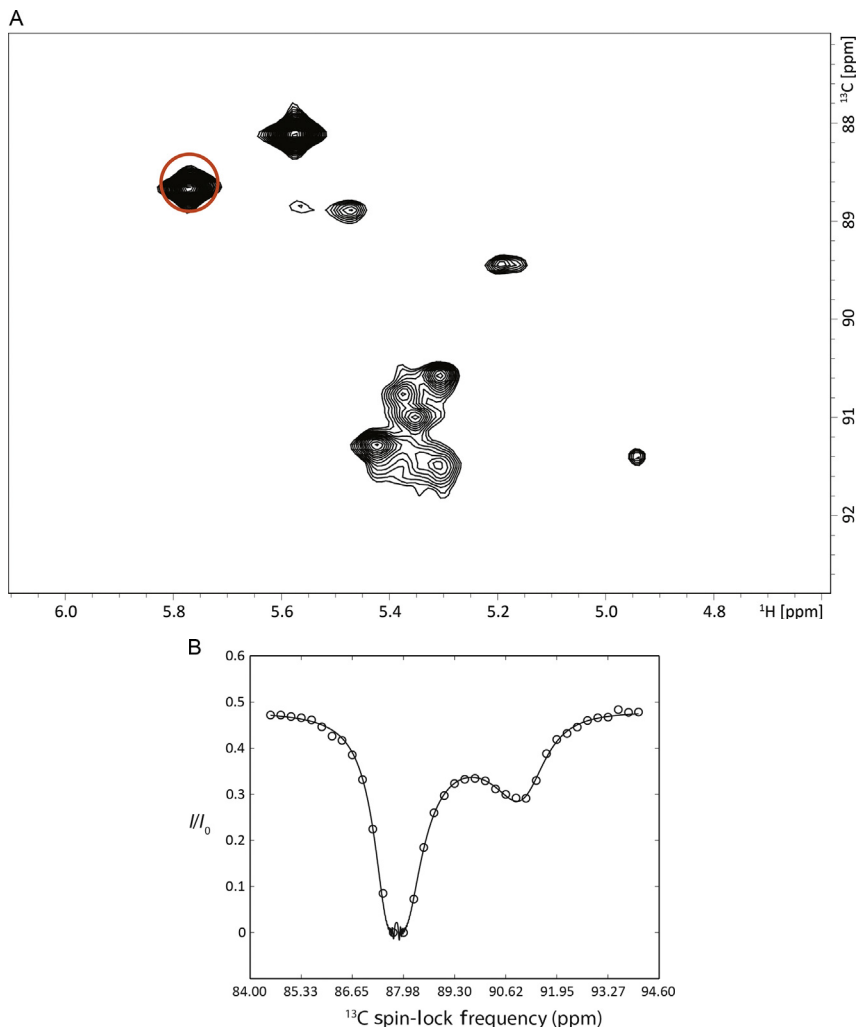


Figure 13 Conformational exchange of a 48 nt fluoride riboswitch probed by ^{13}C CEST NMR spectroscopy (Longhini, LeBlanc et al., 2015). (A) $\text{C1}'$ TROSY HSQC of 6- ^{13}C -selectively UTP-labeled fluoride riboswitch shows peak with CEST profile and carbon chemical shift of minor population shift. (B) CEST Profile of $\text{C1}'$ residue from 2D HSQC CEST of fluoride riboswitch at 35 °C with a spin-lock field of 37.9 Hz. Solid lines are the fits to the experimental data to the Bloch–McConnell equation, assuming a two-site exchange process.

ACKNOWLEDGMENTS

C.K. thanks Martin Tollinger and Thomas Moschen for support in fitting the CPMG RD data. C.K. also thanks Ronald Micura for continuous support. Supported partially by NIH P50 GM103297 (T.K.D.), NMR instrumentation by NSF DBI1040158 (T.K.D.), and the Austrian Sciences Fund (I844 and P26550 to C.K.).

REFERENCES

- Al-Hashimi, H. M. (2007). Beyond static structures of RNA by NMR: Folding, refolding, and dynamics at atomic resolution. *Biopolymers*, *86*(5–6), 345–347.
- Al-Hashimi, H. M., & Walter, N. G. (2008). RNA dynamics: It is about time. *Current Opinion in Structural Biology*, *18*(3), 321–329.
- Alvarado, L. J., LeBlanc, R. M., Longhini, A. P., Keane, S. C., Jain, N., Yildiz, Z. F., et al. (2014). Regio-selective chemical-enzymatic synthesis of pyrimidine nucleotides facilitates RNA structure and dynamics studies. *ChemBioChem*, *15*(11), 1573–1577. <http://dx.doi.org/10.1002/cbic.201402130>.
- Alvarado, L. J., Longhini, A. P., LeBlanc, R. M., Chen, B., Kreutz, C., & Dayie, T. K. (2014). Chemo-enzymatic synthesis of selectively ¹³C/¹⁵N-labeled RNA for NMR structural and dynamics studies. In H. B. A. Donald (Ed.), *Methods in enzymology: Vol. 549* (pp. 133–162). Amsterdam/New York: Academic Press, Elsevier. chapter seven.
- Blount, K. F., & Breaker, R. R. (2006). Riboswitches as antibacterial drug targets. *Nature Biotechnology*, *24*(12), 1558–1564.
- Bouvignies, G., & Kay, L. E. (2012a). A 2D ¹³C-CEST experiment for studying slowly exchanging protein systems using methyl probes: An application to protein folding. *Journal of Biomolecular NMR*, *53*(4), 303–310. <http://dx.doi.org/10.1007/s10858-012-9640-7>.
- Bouvignies, G., & Kay, L. E. (2012b). Measurement of proton chemical shifts in invisible states of slowly exchanging protein systems by chemical exchange saturation transfer. *The Journal of Physical Chemistry. B*, *116*(49), 14311–14317. <http://dx.doi.org/10.1021/jp311109u>.
- Breaker, R. R. (2011). Prospects for riboswitch discovery and analysis. *Molecular Cell*, *43*(6), 867–879. <http://dx.doi.org/10.1016/j.molcel.2011.08.024>.
- Campbell, D. O., Bouchard, P., Desjardins, G., & Legault, P. (2006). NMR structure of varkud satellite ribozyme stem loop V in the presence of magnesium ions and localization of metal-binding sites. *Biochemistry*, *45*(35), 10591–10605. <http://dx.doi.org/10.1021/bi0607150>.
- Chen, B., Zuo, X., Wang, Y.-X., & Dayie, T. K. (2012). Multiple conformations of SAM-II riboswitch detected with SAXS and NMR spectroscopy. *Nucleic Acids Research*, *40*(7), 3117–3130.
- Coppins, R. L., Hall, K. B., & Groisman, E. A. (2007). The intricate world of riboswitches. *Current Opinion in Microbiology*, *10*(2), 176–181.
- Dayie, K. T. (2008). Key labeling technologies to tackle sizeable problems in RNA structural biology. *International Journal of Molecular Sciences*, *9*(7), 1214–1240.
- Dethoff, E. A., Petzold, K., Chugh, J., Casiano-Negroni, A., & Al-Hashimi, H. M. (2012). Visualizing transient low-populated structures of RNA. *Nature*, *491*(7426), 724–728. <http://www.nature.com/nature/journal/v491/n7426/abs/nature11498.html>, supplementary-information.
- Duss, O., Maris, C., von Schroetter, C., & Allain, F. H. T. (2010). A fast, efficient and sequence-independent method for flexible multiple segmental isotope labeling of RNA using ribozyme and RNase H cleavage. *Nucleic Acids Research*, *38*(20), e188.
- Fawzi, N. L., Ying, J., Ghirlando, R., Torchia, D. A., & Clore, G. M. (2011). Atomic resolution dynamics on the surface of amyloid β protofibrils probed by solution NMR. *Nature*, *480*(7376), 268–272. <http://dx.doi.org/10.1038/nature10577>.
- Forsén, S., & Hoffman, R. A. (1963). Study of moderately rapid chemical exchange reactions by means of nuclear magnetic double resonance. *The Journal of Chemical Physics*, *39*(11), 2892–2901. <http://dx.doi.org/10.1063/1.1734121>.
- Fürtig, B., Buck, J., Richter, C., & Schwalbe, H. (2012). Functional dynamics of RNA ribozymes studied by NMR spectroscopy ribozymes. In J. S. Hartig (Ed.), *Methods in*

- molecular biology: Vol. 848* (pp. 185–199). Berlin; Heidelberg, Germany; New York: Humana Press/Springer.
- Haller, A., Souliere, M. F., & Micura, R. (2011). The dynamic nature of RNA as key to understanding riboswitch mechanisms. *Accounts of Chemical Research*, *44*(12), 1339–1348. <http://dx.doi.org/10.1021/ar200035g>.
- Hennig, M., Williamson, J. R., Brodsky, A. S., & Battiste, J. L. (2001). *Recent advances in RNA structure determination by NMR. Current protocols in nucleic acid chemistry*. Hoboken, New Jersey: John Wiley & Sons, Inc.
- Johnson, J. E., & Hoogstraten, C. G. (2008). Extensive backbone dynamics in the GCAA RNA tetraloop analyzed using ¹³C NMR spin relaxation and specific isotope labeling. *Journal of the American Chemical Society*, *130*(49), 16757–16769. <http://dx.doi.org/10.1021/ja805759z>.
- Kieft, J. S., & Batey, R. T. (2004). A general method for rapid and nondenaturing purification of RNAs. *RNA*, *10*, 988–995.
- Kloiber, K., Spitzer, R., Tollinger, M., Konrat, R., & Kreutz, C. (2011). Probing RNA dynamics via longitudinal exchange and CPMG relaxation dispersion NMR spectroscopy using a sensitive ¹³C-methyl label. *Nucleic Acids Research*, *39*, 4340–4351.
- Latham, M. P., Brown, D. J., McCallum, S. A., & Pardi, A. (2005). NMR methods for studying the structure and dynamics of RNA. *ChemBioChem*, *6*(9), 1492–1505. <http://dx.doi.org/10.1002/cbic.200500123>.
- Lebars, I., Vileno, B., Bourbigot, S., Turek, P., Wolff, P., & Kieffer, B. (2014). A fully enzymatic method for site-directed spin labeling of long RNA. *Nucleic Acids Research*, *42*(15), e117.
- Longhini, A. P., Leblanc, R. M., Becette, O., Salguero, C., Wunderlich, C. H., Johnson, B. A., et al. (2015). Chemo-enzymatic synthesis of site-specific isotopically labeled nucleotides for use in NMR resonance assignment, dynamics and structural characterizations, submitted.
- Lu, K., Miyazaki, Y., & Summers, M. (2010). Isotope labeling strategies for NMR studies of RNA. *Journal of Biomolecular NMR*, *46*(1), 113–125. <http://dx.doi.org/10.1007/s10858-009-9375-2>.
- Micura, R. (2002). Small interfering RNAs and their chemical synthesis. *Angewandte Chemie, International Edition*, *41*(13), 2265–2269. [http://dx.doi.org/10.1002/1521-3773\(20020703\)41:13<2265::AID-ANIE2265>3.0.CO;2-3](http://dx.doi.org/10.1002/1521-3773(20020703)41:13<2265::AID-ANIE2265>3.0.CO;2-3).
- Milligan, J. F., Groebe, D. R., Witherell, G. W., & Uhlenbeck, O. C. (1987). Oligoribonucleotide synthesis using T7 RNA polymerase and synthetic DNA templates. *Nucleic Acids Research*, *15*(21), 8783–8798.
- Milligan, J. F., & Uhlenbeck, O. C. (1989). Synthesis of small RNAs using T7 RNA polymerase. *Methods in Enzymology*, *180*, 51–62.
- Mittermaier, A. K., & Kay, L. E. (2009). Observing biological dynamics at atomic resolution using NMR. *Trends in Biochemical Sciences*, *34*(12), 601–611.
- Nelissen, F. H. T., van Gammeren, A. J., Tessari, M., Girard, F. C., Heus, H. A., & Wijmenga, S. S. (2008). Multiple segmental and selective isotope labeling of large RNA for NMR structural studies. *Nucleic Acids Research*, *36*(14), e89.
- Reining, A., Nozinovic, S., Schlepckow, K., Buhr, F., Furtig, B., & Schwalbe, H. (2013). Three-state mechanism couples ligand and temperature sensing in riboswitches. *Nature*, *499*(7458), 355–359. <http://dx.doi.org/10.1038/nature12378>. <http://www.nature.com/nature/journal/v499/n7458/abs/nature12378.html>, supplementary-information.
- Rieder, U., Kreutz, C., & Micura, R. (2010). Folding of a transcriptionally acting PreQ1 riboswitch. *Proceedings of the National Academy of Sciences of the United States of America*, *107*(24), 10804–10809.

- Rinnenthal, J., Buck, J., Ferner, J., Wacker, A., Furtig, B., & Schwalbe, H. (2011). Mapping the landscape of RNA dynamics with NMR spectroscopy. *Accounts of Chemical Research*, 44(12), 1292–1301. <http://dx.doi.org/10.1021/ar200137d>.
- Serganov, A., & Nudler, E. (2013). A decade of riboswitches. *Cell*, 152(1–2), 17–24. <http://dx.doi.org/10.1016/j.cell.2012.12.024>.
- Tzakos, A. G., Easton, L. E., & Lukavsky, P. J. (2007). Preparation of large RNA oligonucleotides with complementary isotope-labeled segments for NMR structural studies. *Nature Protocols*, 2(9), 2139–2147.
- Vallurupalli, P., Bouvignies, G., & Kay, L. E. (2012). Studying “invisible” excited protein states in slow exchange with a major state conformation. *Journal of the American Chemical Society*, 134(19), 8148–8161. <http://dx.doi.org/10.1021/ja3001419>.
- Wawrzyniak-Turek, K., & Höbartner, C. (2014). Deoxyribozyme-mediated ligation for incorporating EPR spin labels and reporter groups into RNA. In H. B. A. Donald (Ed.), *Methods in enzymology: Vol. 549* (pp. 85–104). Amsterdam/New York: Academic Press, Elsevier. chapter four.
- Weininger, U., Respondek, M., & Akke, M. (2012). Conformational exchange of aromatic side chains characterized by L-optimized TROSY-selected 13C CPMG relaxation dispersion. *Journal of Biomolecular NMR*, 54(1), 9–14. <http://dx.doi.org/10.1007/s10858-012-9656-z>.
- Wenter, P., Reymond, L., Auweter, S. D., Allain, F. H. T., & Pitsch, S. (2006). Short, synthetic and selectively 13C-labeled RNA sequences for the NMR structure determination of protein–RNA complexes. *Nucleic Acids Research*, 34(11), e79.
- Wunderlich, C. H., Spitzer, R., Santner, T., Fauster, K., Tollinger, M., & Kreutz, C. (2012). Synthesis of (6-13C)pyrimidine nucleotides as spin-labels for RNA dynamics. *Journal of the American Chemical Society*, 134(17), 7558–7569. <http://dx.doi.org/10.1021/ja302148g>.
- Zhang, Q., Sun, X., Watt, E. D., & Al-Hashimi, H. M. (2006). Resolving the motional modes that code for RNA adaptation. *Science*, 311(5761), 653–656.
- Zhao, B., Hansen, A. L., & Zhang, Q. (2014). Characterizing slow chemical exchange in nucleic acids by carbon CEST and low spin-lock field R1ρ NMR spectroscopy. *Journal of the American Chemical Society*, 136(1), 20–23. <http://dx.doi.org/10.1021/ja409835y>.